THE FE DEPOSIT, WEST-CENTRAL SPAIN: TECTONIC-HYDROTHERMAL URANIUM MINERALIZATION ASSOCIATED WITH TRANSPRESSIONAL FAULTING OF ALPINE AGE

Agustin MARTIN-IZARD[§]

Departamento de Geología, Universidad de Oviedo, Arias de Velasco s/n, E-33005 Oviedo, Spain

Antonio ARRIBAS Sr.

*Departamento de Ingeniería Geológica, E.T.S.I.M., Universidad Politécnica de Madrid,
Ríos Rosas 21, E-28003 Madrid, Spain*

Daniel ARIAS

Departamento de Geología, Universidad de Oviedo, Arias de Velasco s/n, E-33005 Oviedo, Spain

Javier RUIZ

ENUSA, Mina Fé, Apartado 28, E-37500, Ciudad Rodrigo, Salamanca, Spain

Francisco José FERNÁNDEZ

Departamento de Geología, Universidad de Oviedo, Arias de Velasco s/n, E-33005 Oviedo, Spain

ABSTRACT

Primary uranium deposits (uraninite + coffinite + carbonates + "adularia" + iron sulfides) of Mina Fé, in west–central Spain, occur in fault-related rocks. These rocks have been formed by the effect of an aftershock fault cluster at the termination of a major strike-slip fault, the Grafitosa fault. The transpressional shear-zone termination presents two symmetrical brittle dilational jogs with reactivation of old Variscan faults and generation of other new Alpine faults. Lithogeochemical analyses show that the hydrothermal flow associated with the Grafitosa fault mobilized uranium and related elements during pressure solution in carbonaceous slates of the Variscan basement. The orientation of the paleo-stress field in the dilational jogs, deduced from an analysis of fault populations, has shown the range of fault surfaces with favorable orientation for mineral deposition during slate consumption in the restraining bend, which agrees with a extensional setting for the ore deposit. The detailed structural and geochemical data presented here support an Alpine age tectonic-hydrothermal model for the Fé deposit and probably other cases of uranium mineralization of the same type existing in carbonaceous metasedimentary rocks in the Iberian peninsula, most of them uncorformably overlain by Tertiary sedimentary units.

Keywords: ore deposit, tectonic-hydrothermal model, shear zone, dilational jogs, lithogeochemical data, uranium, Fé deposit, Spain.

SOMMAIRE

Les gisements primaires d'uranium (uraninite + coffinite + carbonates + "adulaire" + sulfures de fer) de Mina Fé, par la partie ouest-centrale de l'Espagne, sont situés dans des roches déformées le long de failles. Ces roches ont été déformées par l'effet d'un essaim de failles à la terminaison d'un faille coulissante majeure, la faille Grafitosa. La zone transpressionnelle à la terminaison de la zone de cisaillement présente deux décrochements dilationnels symétriquement disposés, avec réactivation des anciennes failles d'âge varisque et la génération de failles nouvelles lors de l'orogenèse alpine. Des analyses lithogéochimiques montrent que le flux hydrothermal associé à la faille Grafitosa a mobilisé l'uranium et les éléments associés au cours d'une solution sous pression des roches schisteuses carbonacées du socle varisque. L'orientation du champ de déformation dans les zones de décrochement dilationnels à l'époque, telle que déduite à partir d'une analyse de la population de failles, montre l'étendue des surfaces de failles ayant une orientation favorable pour la déposition de minéraux lors de la dissolution des roches schisteuses

---

[§] *E-mail address*: amizard@geol.uniovi.es

dans la zone de plissement sous contraintes, ce qui concorde avec le milieu extensionnel du gisement. Les données structurales et géochimiques détaillées présentées ici étayent le modèle tectonique-hydrothermal d'activité alpine pour expliquer le gisement de Fé, et probablement les autres cas de minéralisation en uranium du même genre dans les roches métasédimentaires carbonacées de la péninsule Ibérique, la plupart d'entre eux recouverts de séquences sédimentaires tertiaires.

<div align="right">(Traduit par la Rédaction)</div>

Mots-clés: gîte minéral, modèle tectonique-hydrothermal, zone de cisaillement, décrochements dilationnels, données lithogéochimiques, uranium, gisement de Fé, Espagne.

INTRODUCTION

The Fé mine exploited the most important uranium deposit in Spain. The fault-related metasedimentary host rocks of the upper Proterozoic to lower Cambrian "schist–graywacke complex" (CEG) are located in the Central Zone of the Iberian Massif (Julivert *et al.* 1972) (Fig. 1). These metasedimentary rocks, together with other Paleozoic formations and bodies of Variscan granite, make up the Variscan basement of the central Iberia, which was unconformably overlain by Tertiary continental clastic and carbonate sedimentary rocks of the Ciudad Rodrigo basin, deposited during the Alpine orogeny.

The uranium deposit was discovered by radiometry in 1957 and commenced production in 1974. Initially, mining activity focused on the zone of supergene enrichment rich in hexavalent uranium minerals. Subsequently, the primary reduced ore was mined.

The annual production until closure, in 2001, was 300 tonnes of U_3O_8, which was obtained by a dynamic leaching in a plant with capacity for 950 tonnes of U_3O_8. The grade of the ore mined was 650 g/t. At present, the non-mineable geological resources in the Fé mine are
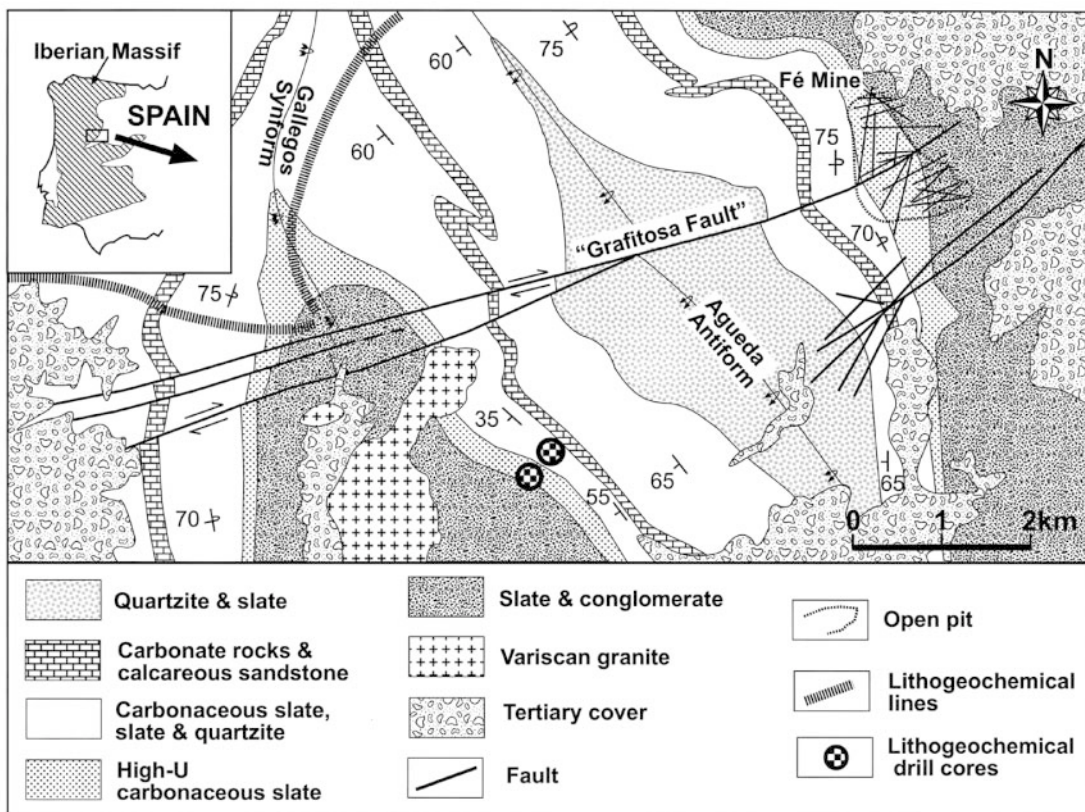
FIG. 1.   Regional geological map of the Fé mine area showing the most important stratigraphic and structural features. High-U carbonaceous slates have a U content of >10 ppm.

in excess of 5,000 tonnes of U_3O_8, using a cutoff grade of 200 ppm. In addition, several other uranium deposits of the same type occur west and north of Ciudad Rodrigo (Zona D, Zona M, Sageras, and Alameda). Total non-mineable geological resources of these deposits amount to more than 19,000 tonnes of U_3O_8, of which 9,000 t comes from the Alameda orebody (Artieda *et al.* 1995, Ruiz *et al.* 1997a, b).

As a reflection of the available geological, mineralogical and geochemical evidence, and the prevailing metallogenic views of the time, the origin of the Fé deposit has evolved from early models based on broadly supergene processes (Arribas 1960, 1962, Fernandez-Polo 1970) to a tectonic-hydrothermal model (Arribas 1985, Both *et al.* 1994) based on a seismic pumping process associated with Alpine tectonism. On the basis of new structural and geochemical data from the Fe deposit and the Ciudad Rodrigo basin, we further support in this paper the tectonic-hydrothermal model by providing details of the tectonic environment and structural deformation in the context of a transpressional shear-zone of Alpine age. Consequently, the emphasis of this study is on a sequential stress analysis of faults associated with the Fé deposit and on a re-interpretation of new and previously available geochemical data (Arribas *et al.* 1984, Martin-Izard 1989, Martin-Izard *et al.* 1999), such as data on leachable uranium and organic carbon, among others.

GEOLOGICAL SETTING

The most important geological features of the Ciudad Rodrigo area have been described by several authors (*e.g.,* Arribas 1962, Arribas *et al.* 1984, Martin Izard 1986, 1989), and summarized by Both *et al.* (1994). A brief description, updated with new data, is given below.

In the Ciudad Rodrigo area, the CEG rocks consist mainly of carbonaceous pelitic and fine-grained psammitic rocks (Fig. 1) metamorphosed to the greenschist facies, in which sedimentary textures are commonly preserved. Interlayered within these rocks are carbonate beds a few meters in thickness (Arribas *et al.* 1984, Martin-Izard 1989).

The CEG rocks were affected by three phases of folding during the Variscan orogeny (Arribas *et al.* 1984, Martin-Izard 1986, 1989). The first phase produced major north- to northwest-trending inclined folds with wavelengths up to 3 km and a well-developed cleavage S_1. The Fé mine is located on the east limb of the Agueda F_1 inclined antiform, which is the major structure in the area (Fig. 1). The second phase folds are approximately east–west-trending, with axial planes dipping steeply north. The wavelengths of the folds are on the scale of meters to tens of meters, and a crenulation schistosity S_2 occurs. This phase of deformation is irregularly distributed, but is widely present in the eastern part of the Fé zone. The inclined folds developed

during D_1 and D_2 phases of deformation have generally associated fractures parallel to the axial planes and along the reverse limbs of the folds. The third phase of deformation was much less intense and produced open north-to northeast-trending folds with a poorly developed axial planar cleavage.

The calc-alkaline granodiorite to quartz monzonites intrude the stratigraphic sequence and belong to the "younger" suite of Variscan granites (Oen 1970). Both the metasedimentary and granitic rocks are cut by late ENE–WSW-trending Variscan fracture zones. The lower to middle Tertiary Alpine orogeny produced further fractures, as well as the rejuvenation of older fractures, and led to the development of phyllonitic and cataclastic breccia zones. The basement rocks and mineralized breccias are locally covered by the unmineralized Oligocene to Miocene terrestrial sedimentary rocks of the Ciudad Rodrigo Basin. In this sense, the mineralization is located beneath the unconformity between the Variscan basement and the Tertiary sedimentary cover.

STRUCTURE OF THE OREBODY

The primary ore displays a strong structural control and is developed around the eastern limit of the Grafitosa strike-slip fault (Fig. 1). The uranium orebody is divided in two sectors (Fé 1 and Fé 3), which are separated by the barren, strongly brecciated graphitic Grafitosa Fault (Figs. 1, 2 and 3a). The breccia gouge is a phyllonitic rock with a well-developed linear fabric where graphite is concentrated in the phyllonitic planes together with minor pyrite. The last movement detected in the Grafitosa Fault developed subhorizontal grooves and steps, which indicate a dextral strike-slip movement.

The uranium ores of the Fé 1 and Fé 3 orebodies are concentrated in the two dilational areas developed around the Grafitosa transpressive shear-zone (Figs. 2, 3a), and occur as narrow veins occupying thin fractures within breccia zones [cataclastic breccia with anastomosed extensional domains (Fig. 3b) in which open spaces are cyclically filled (Figs. 3c, 4) by the uraniferous mineralization]. The geometry of the mineralized breccia zones is very irregular, with changes in thickness, both vertically and horizontally, from several centimeters up to 20 meters, over a few tens of meters (Fig. 3b). The strike of the breccia zones is constant, but on closer inspection changes in both the footwall and the hanging wall. The veins that host the ore range in width from less than 1 mm to a maximum of about 20 cm. The veins also occupy structures resulting from the reopening of the cleavage, fractures, and quartz veins of Variscan age adjacent to the fault breccia.

Several stages of mineral deposition can be observed (Both *et al.* 1994) (Fig. 4). The early stage of hydrothermal mineralization, consisting of veins of ankerite (Fig. 3c, d and e) and iron sulfides with accessory galena and traces of sphalerite and chalcopyrite, has associated limited, but intense chloritization of the wallrock

(Fig. 3f). The second (main) stage, which was the most important in terms of uranium mineralization, involved deposition of K-feldspar of the adularia habit (Fig. 3g), iron sulfides, uraninite (and minor coffinite), calcite and dolomite (Figs. 3c, d, e), followed by limited replacement of K-feldspar by chlorite and hematite. Rarely, additional replacement of chlorite and hematite by uraninite and ankeritic carbonate occurs (Both *et al.* 1994).

The third and final stage was characterized by repeated, episodic deposition of carbonates, iron sulfides, uraninite and coffinite (Figs. 3e, h, i, j). This late hydrothermal stage produced finely laminated, "varve-like" mineralized sediments (Figs. 3j, k). As Both *et al.* (1994) pointed out, ore minerals deposited in the open spaces of the breccia cavities show spectacular stalactitic struc-
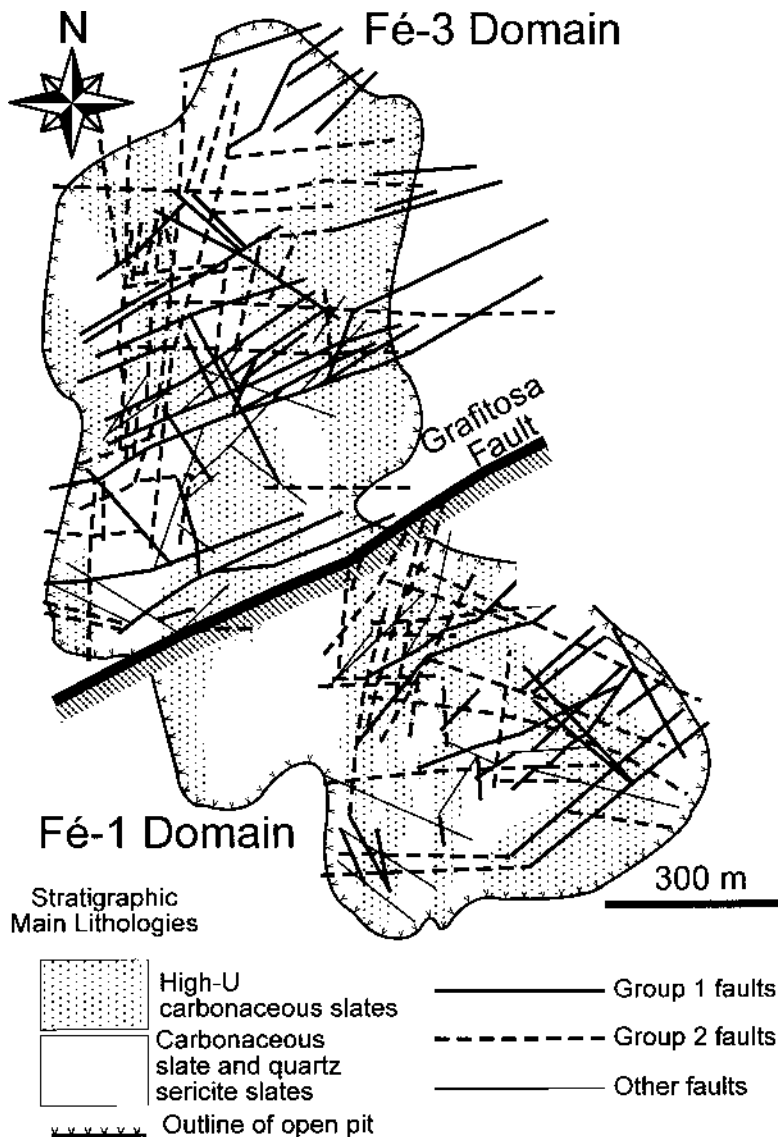
FIG. 2. Geological sketch of the Fé orebody. The two orebodies, Fé 1 and Fé 3, are divided by the Grafitosa fault. The faults affecting both orebodies are distributed in two main groups of conjugate faults, 1 and 2. Note the close relationship between uranium-mineralized faults and stratigraphic levels anomalously enriched in uranium.
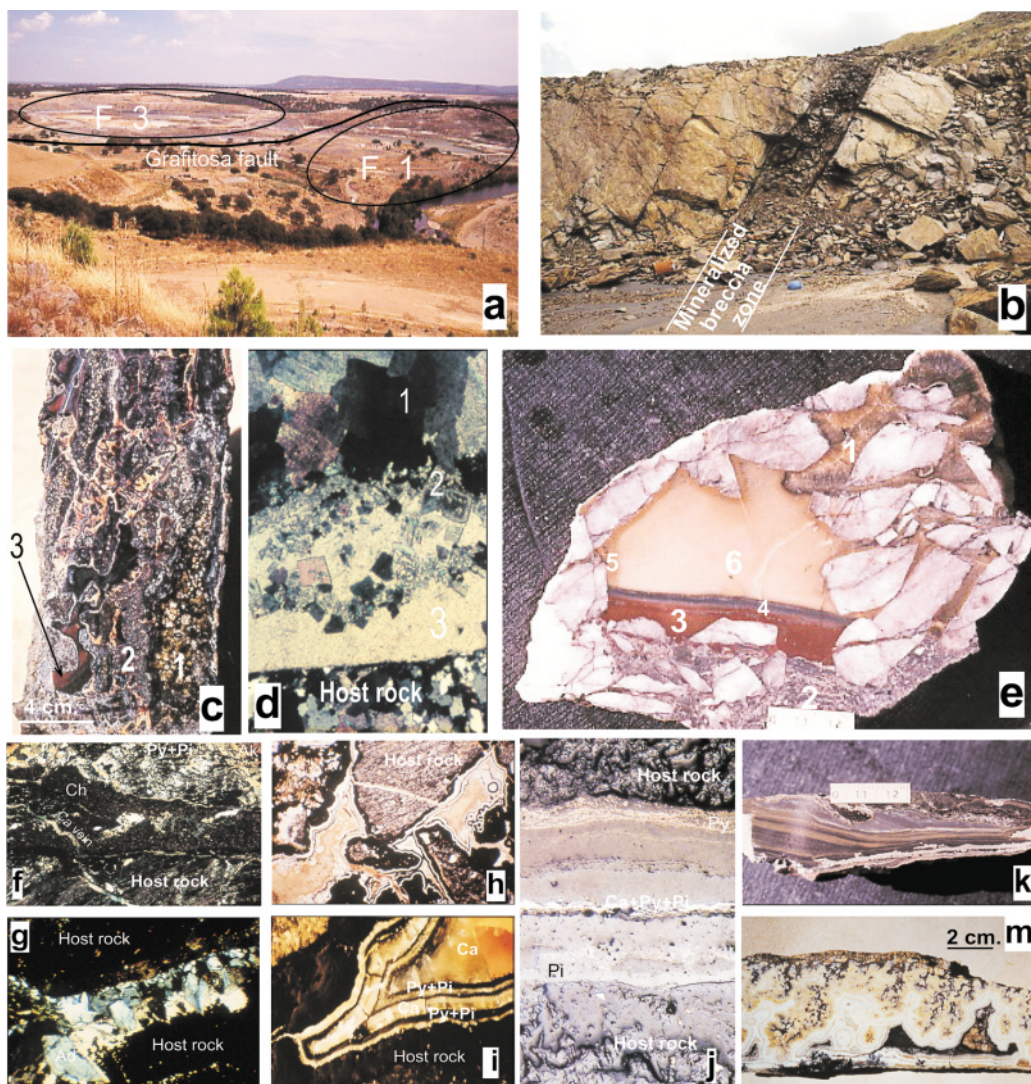
FIG. 3.   Photographs and microphotographs of Mina Fé uranium deposit. a. General view of the Fé mine open pit in which Fé 1, Grafitosa zone and Fé 3 can be distinguished. Both mineralized sections of the deposit are separated by the barren Grafitosa zone. b. Mineralized breccia zone in schist–greywacke complex rocks, Fé 1 ore zone. The geometry of the mineralized breccia zones is irregular, with changes in thickness, both vertically and horizontally. c. Mineralized breccia from Fé 1 ore zone in which three generations of carbonate-rich mineralization can be seen: early (1), well crystallized, main stage (2), and layered late-stage cavity filling (3). d. Three successive generations of carbonate, ankerite (1), dolomite (2) and calcite (3), growing on a quartzite partially replaced by carbonate (thin section, PLX5). e. Brecciated Variscan quartz vein with successive stages of mineralization: 1 early-stage ankerite, 2 main-stage dolomite with pyrite and uraninite, 3 late-stage layered calcite and hematite, 4 late-stage layered calcite, pyrite and uraninite, 5 late-stage iron-rich calcite, and 6 late-stage calcite. f. Chlorite (Ch) alteration of wallrock adjacent to a vein of ankerite (Ak), uraninite (Pi) and pyrite (Py) (thin section, PLX10). g. Thin section of "adularia" crystals filling a microvein in schist (PLX20). h. Thin section of breccia zone in which the fragments of the host rock are successively cemented by alternating bands of carbonate and opaque minerals (pyrite and uraninite) and a final carbonate fills the open spaces in the breccia (PLX5). i. Detailed view in crossed nicols (X20) of the thin section of picture h in which there are alternating bands of carbonate (Ca) and opaque minerals (pyrite and uraninite). j. Polished section of finely laminated sediments containing calcite, pyrite and uraninite (PLX20). k. Polished section of a cavity filled with late-stage carbonate, pyrite and uraninite showing cross-laminated sediments and geopetal textures. m. Stalactitic (upper) and layered (lower) carbonate structures in breccia cavity. The voids between stalactitic and layered structures are filled with late-stage calcite and uraninite.

tures (Fig. 3m) and layering (Figs. 3j, k), including rhythmic layering, graded bedding and cross-bedding.

Figures 2 and 5 show the spatial distribution of the main uranium-bearing veins at the Fé mine. The principal groups of veins strike N–S, ENE–WSW, E–W and NNE–SSW, and correspond to the principal systems of Variscan fractures, which reopened during the Pyrenean phase of the Alpine orogeny.

MINERALIZATION AGE
AND STABLE ISOTOPE ANALYSIS

In the Fé mine area, the uranium mineralization has been dated at 34.8 ± 1.6 Ma by U/Pb analyses of uraninite (Both *et al.* 1994). This age indicates formation of the ore in the middle Tertiary, when the Ciudad Rodrigo Basin was forming and the Variscan basement at its northern border was undergoing deformation related to the Alpine orogeny (Pyrenean phase).

Stable isotope analyses of 26 samples of carbonate gangue, eight of sulfide minerals, two of pyrite and three of graphite from the host rock of the Fé mine were analyzed by Both *et al.* (1994). All the samples have been placed in the relative sequence of mineral deposition (Fig. 4). Calculated $\delta^{18}O_{H2O}$ values range from +16.0 to near 0‰. Values of $\delta^{13}C$ range from –10.5 to –7.2‰ in the carbonates from the early and main stages, and from –10.7 to –23.6‰ in the carbonates from the late stage. Values of $\delta^{34}S$ for pyrite in early-stage mineralization are similar to those of disseminated pyrite in the host rocks, ranging from –8.2 to –26.3‰, but late-stage pyrite has extremely low $\delta^{34}S$ values, ranging from –48.6 to –51.3‰.

SEQUENTIAL FAULT-STRESS ANALYSES

The area surrounding the Fé Mine contains a Variscan basement reworked during Alpine times. The ore is located in extensional structures, mostly filling veins, breccia zones and open spaces. In the Fé area, several populations of faults have been mapped, some of which are mineralized, whereas others are barren. The characteristics and orientation of the faults indicate that most of them are Variscan faults that were reworked in Alpine times during the development of the transpressive Grafitosa Fault Zone. To the north and south of the Grafitosa Fault, two dilational jogs developed. The Variscan faults were reactivated in these dilational areas. During later transpressional development, the faults with suitable orientation to the stress state were opened, and the rest were closed.

The "slip model" of brittle deformation (Reches 1983) has been applied in the Fé mine area in order to constrain the "stress state" during the genesis of the orebody. This approach allows us to determine the directions of principal stress and to establish whether their orientations are in accordance with the orientations of the mineralized faults. However, the single approach of the "slip model" using the statistical analyses of the fault trends is not suitable for areas of polyphase deformation, such as in the Ciudad Rodrigo basin. In fact, this method is only adequate for a homogeneous basement, where deformation is accommodated by displacement along the slip plane of sets of suitably oriented faults, assuming homogeneous strain and stress. Obviously, this ideal case does not suit the geological framework of the Ciudad Rodrigo area.
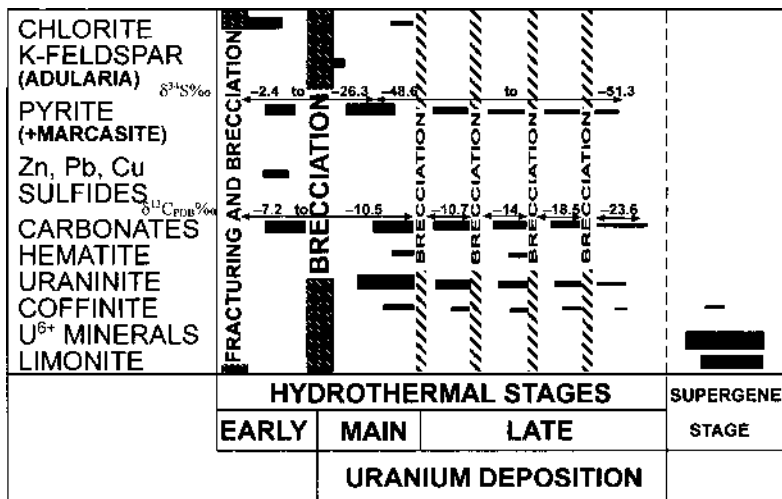
FIG. 4.   Paragenetic sequence of mineral deposition (modified after Arribas 1985). Values of $\delta^{13}C$ and $\delta^{34}S$ have been placed in the relative sequence of mineral deposition.
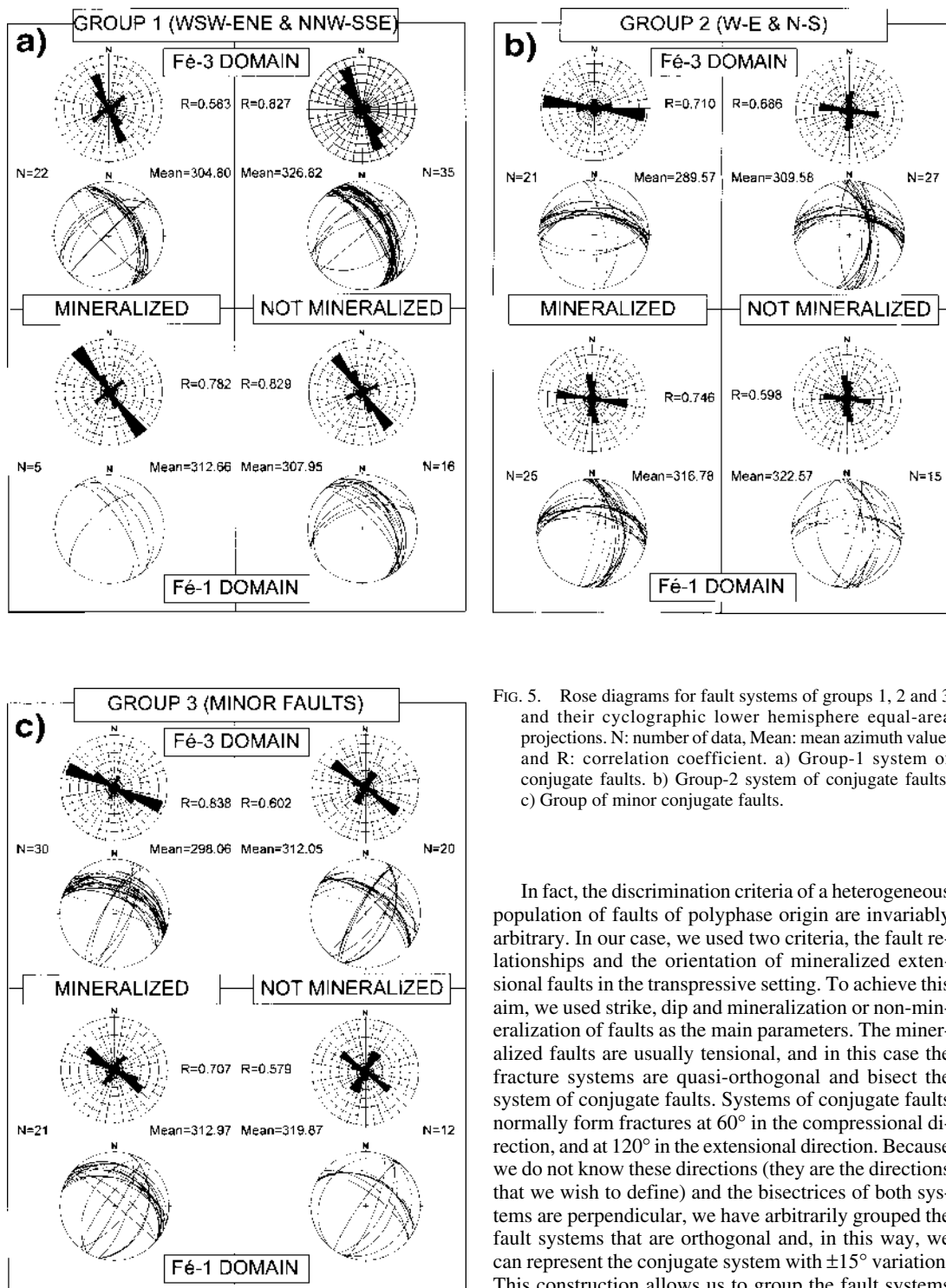
FIG. 5.   Rose diagrams for fault systems of groups 1, 2 and 3 and their cyclographic lower hemisphere equal-area projections. N: number of data, Mean: mean azimuth value, and R: correlation coefficient. a) Group-1 system of conjugate faults. b) Group-2 system of conjugate faults. c) Group of minor conjugate faults.

In fact, the discrimination criteria of a heterogeneous population of faults of polyphase origin are invariably arbitrary. In our case, we used two criteria, the fault relationships and the orientation of mineralized extensional faults in the transpressive setting. To achieve this aim, we used strike, dip and mineralization or non-mineralization of faults as the main parameters. The mineralized faults are usually tensional, and in this case the fracture systems are quasi-orthogonal and bisect the system of conjugate faults. Systems of conjugate faults normally form fractures at 60° in the compressional direction, and at 120° in the extensional direction. Because we do not know these directions (they are the directions that we wish to define) and the bisectrices of both systems are perpendicular, we have arbitrarily grouped the fault systems that are orthogonal and, in this way, we can represent the conjugate system with ±15° variation. This construction allows us to group the fault systems that have been analyzed.

To define the stress state during the formation of the orebody, 249 faults from the Fé 1 and Fé 3 mines have been analyzed by studying the trends of conjugate faults, as predicted by the slip model, and classified. These faults are mostly displaced Variscan faults, located in the two dilational jogs developed around the Grafitosa Alpine transpressive shear-zone. The methodology that was employed consisted of the following steps: (a) the fault populations were grouped into approximately orthogonal sets of faults according to the field information (Fig. 2); (b) the sequence of fault movements was defined by studying the movement deduced from kinematic indicators on fault surfaces and minor structures; (c) the faults were classified in the two groups of conjugate faults defined in (a) and (b), and also in a third group of unclassified faults. Then, the fault characteristics and their relationships with the Fé orebody (Fé 1 and Fé 3) were established in order to define the stress field during the ore formation, and to determine whether the results support the proposed genetic model.

This approach assumes that quasi-orthogonal sets of faults are conjugate, but this assumption is impossible to prove because the Variscan faults were reactivated during the transpressive Alpine movement. The final result of polyphase deformation is that all "conjugate sets" have moderate to shallow plunge (NE to NNE), suggesting they have a dip-slip component.

Using the reserves of uranium ore as a criterion, the faults were grouped in two main areas, to the north and south of the strike-slip transpressive Grafitosa Fault. These areas correspond, respectively, to the Fé 3 and the Fé 1 mine, the latter being richer in mineralized faults. Analyzing the fault-orientation map (Fig. 2) and related stereoplots (Fig. 5), one can see that both domains contain two groups of orthogonal faults with the same preferred orientation. The first group consists of faults trending WSW–ENE, which have the same orientation as the Grafitosa Fault, and are conjugate with respect to faults trending NNW–SSE (Fig. 5a). The second group is made up of conjugate faults trending W–E and N–S (Fig. 5b). Both trends appear to dip steeply, and the uranium mineralization appears to have occurred dominantly along N–S and NNW–SSE trends, which have the same trend as the F1 folds.

To define the sequence of movements, the cross-cutting relationships between the different sets of faults were studied. All the sets of faults were activated several times by sliding or by opening of the fault surfaces, although it was not possible to infer a timing relationship. Nevertheless, we can deduce two main movements on the slickensided surfaces of some faults of groups 1 and 2.

Using the previously defined method of classification, the population of faults has been divided into three groups. The third group is composed of faults that are not visible at the map scale, but are important at the outcrop scale, owing to their abundance and the presence of uranium mineralization.

The three groups of faults defined above have the following characteristics.

(i) The first group (which is composed of faults oriented WSW–ENE and NNW–SSE) has the NNW–SSE-trending faults dipping homogeneously 50°NE, with these faults occurring three times more frequently than the WSW–ENE faults, which dip NNW at variable angles (Fig. 5a). The NNW–SSE-trending faults display a gentle anticlockwise rotation (about 10°) in the Fé 3 domain in relation to the Fé 1 domain (Fig. 5a), which is consistent with a dextral strike-slip displacement of the Grafitosa Fault. The structural orientation of these faults allowed their opening and subsequent mineralization during the movement of the Grafitosa Fault, as suggested by the data analyzed.

(ii) The W–E-trending faults of the second group, which is composed of faults oriented W–E and N–S, have an orientation correlation coefficient $R = 0.746$ amongst the mineralized faults. The non-mineralized faults (Fig. 5b) have no preferred orientation. This fact suggests that the second group of faults had formed before the first group and was reactivated during ore formation, because W–E trends are mainly mineralized and they are in the open quadrant of the transpressional shear-zone (Fig. 6).

(iii) The third group (indeterminate faults on the structural map) is composed of WNW–ESE-oriented faults dipping 45°N, perpendicular to SSW–NNE-oriented faults of variable dip. No rotations are found between the Fé 3 domain and the Fé 1 domain. R is 0.838 for the mineralized faults, and the WNW–ESE-oriented faults and the NNE–SSW-oriented faults are found in relation to the non-mineralized faults (Fig. 5c). Consequently, we can deduce that the third group of faults is syngenetic with ore formation. The field stress according to model of Reches (1983) has a stretching component oriented N70°W, gently west-dipping. The normal shortening component (σ_1) has an adequate position for the activation of the dextral strike-slip movement of the Grafitosa fault during the ore formation.

The first general movement on WSW–ENE and E–W trends was normal, as demonstrated by the fact that most of the entire southern block has slickensided surfaces that trend 170° and plunge 30–45° (group 2, Fig. 5). Striae and grooves on the fault surface show normal movement of the hanging wall. According to the field evidence, the overlapping of subperpendicular shear fibers on a similar oriented slickenside surface suggests that later motion along the fault was strike-slip. The motion along the Grafitosa Fault is consistent with this movement. The Grafitosa Fault and the faults parallel to it have no uranium mineralization.

Finally, we have attempted to model the field stress for groups 1 and 2 (Fig. 6). The position of σ_1 before ore formation may be NW–SE, as shown by the characteristics of the second group of faults. However the azimuths of the first group of faults, which were also formed before the ore, are more consistent with the po-
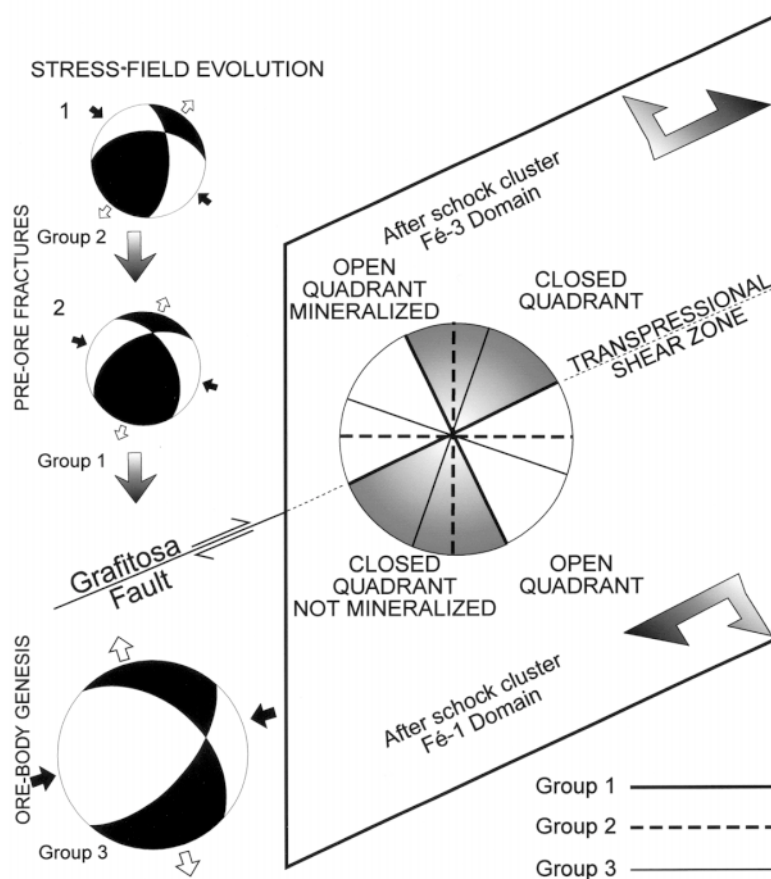
FIG. 6. Structural model of the Fé mine area during the orebody genesis, when group-3 conjugate faults were formed, and prior to that, when group-1 and group-2 conjugate faults were formed. The sequential analyses of faults allowed us to identify the location of the stress field during the ore-genesis process and before it. White arrows show the direction of horizontal stretching, and black arrows show the direction of horizontal shortening. The simplified lower-hemisphere equal-area projections show the extension field in black and the compression field in white.

sition of the field stress inferred at the time of mineralization. This fact suggests an anticlockwise rotation of σ_1 from N45°W to N70°W.

The orientation of the stress field during the ore formation in the transpressional area of the Fé mine allows us to predict the range of fault surfaces with suitable orientation for mineralization, because they invariably are open during the strike-slip movement of the Grafitosa Fault. In contrast, the fault orientations in the stretching field were not mineralized at all or only slightly so (Fig. 6). Therefore, the NE-oriented faults closed during right-lateral movement of the Grafitosa Fault, and NW faults opened. This model is highly consistent with the distribution of mineralized and non-min-

eralized faults (Figs. 3a, b, c) and strongly supports validation of the proposed genetic model.

LITHOGEOCHEMISTRY

Regional lithogeochemical studies were previously carried out by Arribas *et al.* (1984) and Martin-Izard (1989). These authors took more than 800 samples in three regional profiles and two drill cores far from mineralized areas (Fig. 1). They showed that in the Ciudad Rodrigo region, quartzites, conglomerates, schist and calc-silicate rocks have a uranium content of less than 15 ppm (average 4 ppm), whereas more than 15% of the carbonaceous slates, which constitute about 40% of

the stratigraphic sequence, have uranium contents ranging from 30 to 200 ppm (average 60 ppm). In this 15% of uranium-anomalous carbonaceous slates, more than 60% of the uranium is easily leachable (uranium extracted from rock powder by leaching with 7 wt.% HNO_3 at 80°C for two hours under oxidizing conditions). In these samples containing anomalous uranium, there is a significant correlation between uranium and amount of organic carbon (R = 0.675). As these authors pointed out, most of the high-U samples come from the same stratigraphic horizon, which is detected in the different geochemical profiles as well as in the drill cores (Fig. 1). In addition, 60% of the carbonaceous slates are anomalous in Cu, Zn and Ni.

Moreover, Martin-Izard (1989) detected a clear difference in behavior of S in organic-matter-rich samples from the surface and from drill-cores. Whereas the samples from the surface have a great dispersion and low S content (up to 0.8 wt%, average 0.07 wt%), samples from drill-cores have a high S content (up to 4.5 wt%, average 1 wt%) which correlates with organic carbon (R = 0.6), and is evidence of partial oxidation and mobilization of S in samples from the surface. In this way, the most representative and accurate samples are unaltered ones from drill-cores and open pits. There are no important differences between amount of organic C and U in samples from the surface and from drill-cores, proving that C and U contents are much less alterable than S.

Taking into account all these data (Table 1) and the uranium-remobilization hypothesis, more than 100 samples were collected from the Fé area to test the behavior of uranium and organic carbon during the remobilization of uranium from the carbonaceous U-rich slates during Alpine tectonic events (34.8 ± 1.6 Ma,

Both *et al.* 1994). Unaltered, unweathered samples were taken from the Fé drill cores and the Fé open pit. We took three types of samples: rocks not affected by brecciation (normal slates and carbonaceous slates), rocks close to the Grafitosa breccia zone (partially phyllonitic non-cataclastic slates and carbonaceous slates), and the Grafitosa breccia zone (phyllonitic carbonaceous slates).

We analyzed each sample for total U, leachable U by spectrometry and total C, organic C and S by LECO at ENUSA in Spain, and Cu, Zn, Ni and Fe by X-ray energy dispersion with a Kevex instrument at the University of Santiago (Spain). To check the quality of analyses, a selected group of duplicate samples were analyzed at the ACTLABS laboratory in Canada. Concentrations of total C, organic C and S were established with a LECO apparatus, and the other elements, by ICP–MS analysis (Table 1).

In the Fé area, the easily leachable uranium accounts for only 40% of the total (20% less than in regional geochemical studies: Arribas *et al.* 1984, Martin-Izard 1989). A plot of organic carbon *versus* total uranium of samples as established from previous regional geochemical studies and the Fé area is shown in Figure 7. Comparison of these data allow, in samples from the Fé mine, the definition of three groups of samples, A, B, C. Group A is the reference population previously obtained by Arribas *et al.* (1984) and Martin-Izard (1989) for the CEG rocks. The other two sample populations have low and very low uranium contents in relation to organic carbon content. All samples of the B population come from partially tectonized carbonaceous slates, whereas the C population corresponds to samples from the Grafitosa fault in the Fé mine.

With regard to other elements sought, such as Cu, Zn and Ni, which are anomalous in carbonaceous slates,

TABLE 1. MEAN CONCENTRATION AND STANDARD DEVIATION OF ELEMENTS IN SAMPLES OF THE CIUDAD RODRIGO AREA, WEST-CENTRAL SPAIN

Type of samples and number Element	Surface samples			Drill-core samples			Mina Fé samples		
	All samples (800) (*)	Carbonaceous slates (330) (*)	U-rich carbonaceous (86) (*)	All samples (182) (*)	Carbonaceous samples (86) (*)	U-rich carbonaceous slates (29) (*)	All samples (100) (*)	Samples outside the Grafitosa fault (58)	Samples from Grafitosa fault (13)
U total (ppm)	4.6 (5.4)	5.4 (6.8)	13.1 (10)	5.4 (6.6)	8.0 (8.4)	13.4 (7)	7 (4.6)	7.4 (5)	4.8 (4)
U labile (ppm)	2.3 (3.1)	2.7 (3.6)	6.5 (5.5)	3.3 (5)	4.8 (6.7)	8 (4.8)	2.7 (3.4)	2.7 (3.8)	2.6 (3.1)
C organic (%)	0.35 (0.5)	0.5 (0.6)	0.5 (0.6)	0.44 (0.5)	0.53 (0.5)	0.5 (0.4)	0.5 (0.5)	0.3 (0.2)	1.9 (0.6)
C total (%)	0.58 (1.2)	0.5 (0.6)	0.54 (0.6)	0.53 (0.5)	0.6 (0.5)	0.54 (0.4)	0.8 (0.7)	0.5 (0.4)	2.3 (0.8)
Cu (ppm)	45 (20)	48 (20)	45 (19)	46 (14)	53 (14)	54 (17)	40 (31)	41 (35)	46 (16)
Zn (ppm)	100 (39)	97 (33)	99 (34)	110 (23)	115 (17)	120 (20)	110 (43)	119 (40)	120 (36)
Ni (ppm)	34 (18)	32 (18)	34 (19)	47 (11)	48 (12)	49 (11)	44 (14)	43 (14)	52 (11)
S (%)	0.07 (0.07)	0.09 (0.09)	0.09 (0.1)	1.4 (0.8)	1.8 (1)	1.51 (0.9)	1.6 (1.1)	1.3 (0.8)	2.1 (0.8)
Fe (%)	6.7 (3)	7 (1.6)	7 (1.6)	7.5 (1)	7.2 (0.9)	6.9 (1)	7 (1.7)	7.1 (1.8)	7.5 (1.8)

* Data from Martin-Izard (1989).
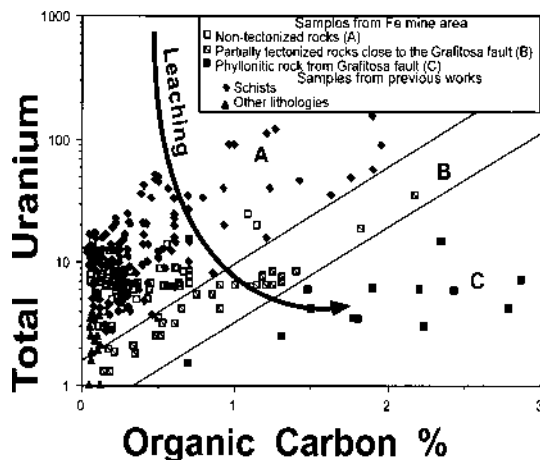
FIG. 7.   Scatter plot of organic carbon *versus* total uranium in samples from the Fé area and from previous investigations. All samples from the Fé area are non-mineralized carbonaceous and non-carbonaceous slates and tectonized carbonaceous slates from the "Grafitosa" fault. Samples from previous studies are mostly slates and carbonaceous slates, and minor quarzites, conglomerates, as well as two calc-silicate rocks. The two calc-silicate samples have 1 ppm of U. Quartzites and conglomerates have less than 5 ppm. In samples from the Fé area, three families can be distinguished, A, B and C. An arrow indicates the proposed process of U leaching and increase in organic carbon from non-tectonized slates (family A) through partially brecciated slates (family B) to samples from the Grafitosa breccia gauge (family C).

their contents are approximately the same in the different types of rocks. Only a small increase in the average content of these elements can be detected in type-C samples. This indicates that the conditions of uranium mobilization are not adequate for mobilizing base metals. Thus Cu, Zn and Ni remain in the tectonized rocks. This fact agrees with the paragenetic sequence at Mina Fé; small amounts of sphalerite and chalcopyrite can be found only in the early stage (Fig. 4), invariably before the deposition of uranium minerals. At the stage of uranium mineral deposition, the only sulfides present are pyrite and marcasite, carbonates being the most abundant minerals in the gangue. Uranium was probably transported in the hydrothermal fluid as carbonyl ions in neutral to alkaline pH conditions (Cuney *et al.* 1991); such conditions are not appropriate for the transport of Cu or Zn.

GENESIS OF THE FÉ URANIUM DEPOSIT

Stable isotope analyses of carbonate gangue minerals from the Fé mine (Both *et al.* 1994) suggest the mineralization formed from a hydrothermal system

dominated by water of meteoric origin that underwent extensive isotopic exchange with the CEG rocks. Values of $\delta^{13}C$ in the carbonates from the early and main stages (–10.5 to –7.2‰) and in the carbonates from the late stage (–10.7 to –23.6‰) indicate that carbon was initially derived by dissolution of carbonate, and in the later stages, from carbonaceous material in the CEG rocks. A decrease of $\delta^{13}C$ to very low values in the final stages of mineralization indicates an increasing component from the carbonaceous material. Values of $\delta^{34}S$ for pyrite in early-stage mineralization (–8.2 to –26.3‰) are similar to those of disseminated pyrite in the host rocks, but late-stage pyrite has extremely low $\delta^{34}S$ values (–48.6 to –51.3‰), which suggests biogenic deposition from a low-temperature fluid.

Lithogeochemical data suggest that the uranium was leached from the slates with elevated uranium, within the Grafitosa transpressional shear-zone. Other elements that are present in anomalous amounts in the carbonaceous slates include S and C; these elements may also have been mobilized with uranium and are also present in the U mineralization of the Fé mine as sulfides and carbonates that evolved from ankerite during the early stage to dolomite during the main stage, and then to calcite during the late stages (Both *et al.* 1994). Only in the early stage, within which there are no U minerals, is there precipitation of small amounts of other sulfides such as galena, sphalerite and chalcopyrite, indicating that only in this early stage could some Cu, Zn or Pb be mobilized. During the U-deposition stages, no Cu, Zn or Pb mobilization occurred, these elements remaining in the Grafitosa Fault gauge.

On the basis of current geological knowledge of the Fé deposit, the most appropriate model for the origin of the mineralization involves hydrothermal systems operating in response to Alpine tectonic activity in the lower to middle Tertiary. As suggested by Arribas (1985), the hydrothermal systems may have been driven by a process similar to seismic pumping, first proposed by Sibson *et al.* (1975).

Uranium and associated elements, such as Mg, Ca, K, Fe, Mn, C and S, may have been leached from the metasedimentary rocks of the Variscan basement in response to pressure solution. If this was the case for the Fé orebody, the uranium and other components were derived largely by dissolution from carbonaceous slates, with transport of uranium in the form of a uranyl carbonate complex, and deposited in a reducing environment in the fracture and breccia zones in the CEG. In this situation, the barren ENE-trending Grafitosa Fault Zone, which bisects the Fé deposit and separates the orebody in two zones, Fé 1 and Fé 3 (Fig. 2), could be the result of Alpine shearing in a transpressional overlap, which develops two dilational jogs where the ore is found. This term was first used by Harland (1971) to describe deformation arising from the oblique convergence of plates. Transpression is considered by Sanderson & Marchini (1984) as a wrench or trans-

current shear accompanied by horizontal shortening across, and vertical lengthening along the shear plane.

The formation of this transpresional shear-zone could be favored owing to the complexity of Variscan tectonic activity in the Fé mine area, with superposition of different tectonic episodes. Thus, the anisotropy of the area is greater than in the rest of the zone, with many structural discontinuities, which would favor the refraction of the Grafitosa Fault during Alpine times, and the development of the transpressional fracture-zone.

In the Fé mine, the Grafitosa Fault presents a deflection in the trace of the continuous dextral strike-slip fault (Fig. 1) that produced an antidilational jog, which probably implies locking. Thus, we have calculated a lateral displacement of 250 m on the Grafitosa Fault west to the Agueda Anticline, whereas around the Fé mine, this displacement is less than 10 m (Fig. 1). The shortening across the zone results in change in area that must be compensated by vertical thickening in order to conserve volume. This process was accompanied by pressure-solution and mobilization of soluble elements provoked by the more intense strain. An aftershock cluster that controlled the subsidiary deformation and fluid redistribution associated with the pressure solution caused by earthquake rupturing developed around the transpressional jog generated by the bend in the Grafitosa Fault (Fig. 8). This process provoked a distributed crush brecciation, involving microfracturing over a broad region around the antidilational jog (Sibson 1985, 1989). In the Fé area, the old Variscan fault-zones were preferentially reactivated and led to the generation of new fractures in all directions (Figs. 2, 8). Many of these characteristics can be seen in the San Andreas fault zone (Harding 1974, Sylvester & Smith 1976), and in the Najd fault system, Saudi Arabia (Moore *et al.* 1979). The greater structural complexity associated with aftershock clusters developed in transpressional shear-zones helps to explain why they are preferred sites for mineralization (Sibson 1989).

In the Fé mine, the restraining bend of the Grafitosa Fault affected carbonaceous slates with a high background concentrations of uranium (Fig. 1). The displacement of the Grafitosa Fault was 250 m, affecting in the transpressional jog a prism of carbonaceous slate with a minimum dimension of 700×60 m in plan, and 2,500 m in depth (Fig. 8). This model supposes a consumption of 294 million tonnes of slates (density 2.7 g/cm^3) with uranium content of 60 ppm. Accepting a mobilization of 60%, the uranium available would be 10,500 tonnes of U (12,500 tonnes of U_3O_8), approximately 80% of the Fé resources. The additional 20% of the U resources were possibly extracted from secondary transpressional faults developed in the aftershock cluster. Thus, the carbonaceous slates in the Fé mine show 20% depletion in U in comparison to the regional values.

EVOLVING GENETIC MODELS OF THE FÉ DEPOSIT: COMPARISON WITH OTHER URANIUM DEPOSITS

Compared to uranium deposits elsewhere, the Fé deposit in western Spain presents some similarities in setting and style of mineralization with large, rich uranium deposits in northern Australia (in the East Alligator River region of the Pine Creek geosyncline) and central Canada (in the Athabasca region of Saskatchewan). In these three regions, economic uranium mineralization has a structural control and an affinity with carbon-rich horizons and occurs below major unconformities within intracratonic basins. However, unlike the unconformity-type uranium deposits of Canada and Australia, the sedimentary cover in the Ciudad Rodrigo basin is not mineralized (Martin-Izard *et al.* 1999).

The similarities in geological features among these uranium deposits have led to a similar evolution in terms of genetic models proposed for their origin over the past three decades. For the Canadian and Australian unconformity-related deposits, four main genetic models have been proposed so far. In the early 1970s, a supergene or erosional model was originally proposed by Knipping (1971, 1974). This model involved leaching of uranium and other metals from Lower Proterozoic and Archean basement rocks by groundwaters during weathering and regolith formation. The metals were then remobilized and precipitated at redox boundaries, such as carbonaceous metasediments, before the deposition of the middle Proterozoic red-bed sediments of the Athabasca Basin. In this context, Dahlkamp & Tan (1977) and Dahlkamp (1978) proposed later a complex multiphase model, that involved further mobilization of uranium postdating the deposition of the Athabasca sediments. In 1974, Little proposed a hydrothermal model, and suggested that the uranium mineralization was caused by ascending solutions whose upward movement became blocked at the pre-Helikian unconformity. Later on, Von Pechman (1985) envisaged a metamorphic model, in which mineralization was generated by hypogene hydrothermal solutions originated during metamorphism of Lower Proterozoic rocks.

Finally, the diagenetic–hydrothermal model proposed by Hoeve (1978), Hoeve & Sibbald (1978), Pagel (1977) and Hoeve *et al.* (1980) is now the most commonly used to account for the formation of the Athabasca Basin unconformity-related uranium deposits. This model requires mixing of highly saline, descending basinal fluids with variably reduced, ascending basement fluids at temperatures between 180 and 220°C. After 1984, modifications to this model were proposed by Hoeve & Quirt (1984, 1987), Wilson & Kayser (1987), Kotzer & Kayser (1995), and Fayek & Kyser (1997), who argued that the transport and pre-

1) PRE-FAULT STAGE

main source
region (80%U)

Carbonaceous
slates (60 ppm U)

secondary source
region (20%U)

2) SYN-FAULT STAGE

Transpressional jog

Dilational cluster

Dilational
cluster

3) LATE-FAULT STAGE

Open pit boundary

Transpressional
jog

Dilational cluster

Dilational
cluster

1 km
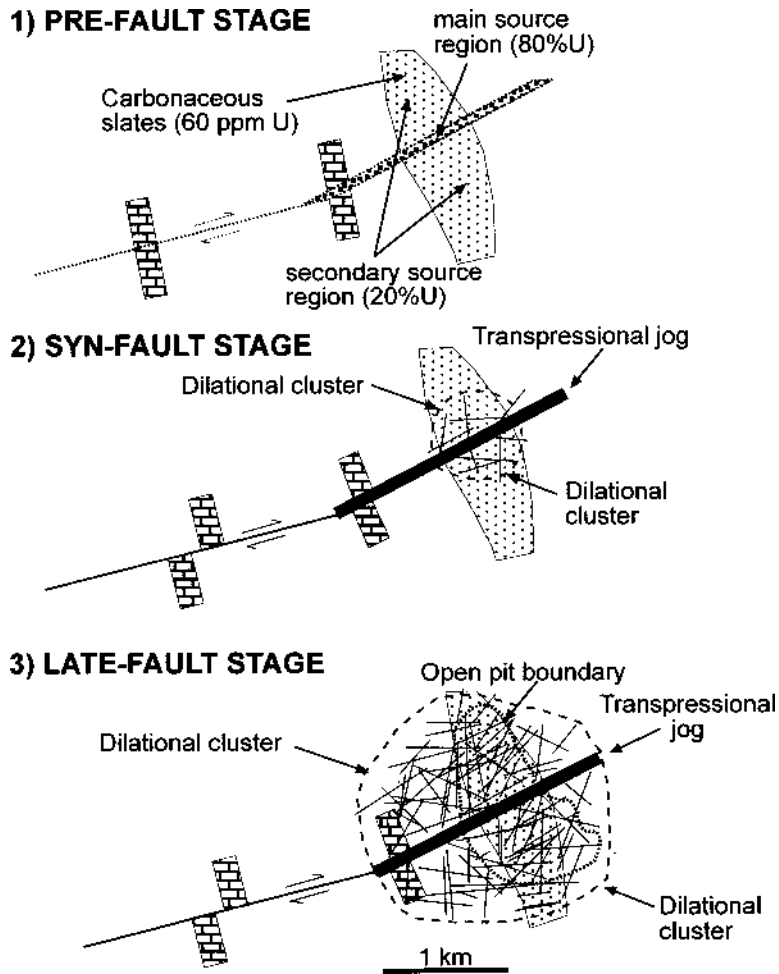
FIG. 8. Genetic model proposed for the deposition of the uranium mineralization in the Fé orebody.

cipitation of uranium were related, as McCready *et al.* (1999) summarized, to basin paleohydrology, large-scale reactivated structures in the basement, fluid flow, and physicochemical traps.

In the case of the unconformity-related uranium deposits of northern Australia, the ores also postdate the Middle Proterozoic sediments of the Kombolgie Formation, which overlies the Lower Proterozoic to Archean chlorite and graphite schists of the basement, namely those of the deposit-hosting Cahill Formation. Two genetic models have been proposed to explain the origin of these deposits: the metamorphic–hydrothermal (Hegge & Rowntree 1978), which suggests that ore fluids originated during metamorphism of uraniferous granites and metasediments in the basement, and the

magmatic–hydrothermal (Binns *et al.* 1980), which calls upon convection driven by post-tectonic radiothermal granites.

As additional evidence was collected through the study of new exploration and mining data, our genetic models for the Spanish Fé uranium deposit evolved as follows: 1) supergene release of uranium from Variscan granites (Arribas 1960, 1962, 1970), 2) weathering and erosion during Pliocene peneplanation (Fernandez-Polo 1970, Matos Dias & Soares de Andrade 1970), 3) segregation by leaching of uranium from plutonic rocks as a consequence of late Variscan or Alpine tectonic activity, 4) tectonic–hydrothermal activity, initially proposed by Arribas (1985) and Booth *et al.* (1994), and which is the model developed further here. Compared to the

various genetic models mentioned above, it seems clear that neither the magmatic and metamorphic, nor the diagenetic–hydrothermal models can be applied to explain the origin of the Spanish deposit. The age of this mineralization, 34.8 ± 1.6 Ma, corresponding to the Lower Oligocene, rules out any relationship with either Hercynian metamorphic processes or granite intrusions, or with the diagenesis of the overlying Tertiary sediments. As for the supergene or erosional model, no weathering of the basement took place prior to the deposition of the cover.

CONCLUSIONS

The Fé orebody developed in a transpressional shear-zone of Alpine age. The Grafitosa dextral strike-slip fault represents a compressional jog in the Fé area that affected carbonaceous slates with a high background concentration of uranium. A minimum of 294 million tonnes of carbonaceous slates were contained in the restraining bend; the mobilization of 10,500 tonnes of U by hydrothermal fluids represents around 80% of the Fé geological reserves (cutoff 200 ppm). The additional 20% of U in the geological reserves were extracted from secondary transpressional faults developed in the two aftershock cluster or dilational jogs formed around the transpressional overlap of the Grafitosa Fault. The development of the dilational jogs caused the formation of a zone of crush brecciation with the reactivation of the old Variscan faults and the generation of new Alpine faults in all directions. These fractures and breccias permitted the circulation of the fluids moving by pressure solution and the deposition of the uranium ores. Similar processes were described in the San Andreas Fault Zone and in the Najd Fault System.

Later on, the basement rocks and mineralized breccias and veins became covered in places by continental Tertiary sediments of the Ciudad Rodrigo Basin. In this way, the mineralization is located underneath the unconformity between the Variscan basement and Tertiary cover, and it could be compared to Proterozoic unconformity-type uranium deposits of Canada and Australia. Nevertheless, in the Ciudad Rodrigo Basin, the sediments of the cover are not mineralized, contrary to the case in the unconformity model.

ACKNOWLEDGEMENTS

REFERENCES

ARRIBAS, A. (1960): Mineralogy of Spanish uranium deposits. *22nd Int. Geol.Congress* (*Copenhagen*) **15**, 98-108.

_____ (1962): Mineralogía y metalogenia de los yacimientos españoles de uranio: las pizarras uraníferas de la provincia de Salamanca. *Estudios Geológicos* **18**, 155-172.

_____ (1970): Las pizarras uraníferas de la provincia de Salamanca. *Studia Geologica Salmanticensia* **1**, 7-37.

_____ (1985): Origen, transporte y deposición del uranio en los yacimientos en pizarras de la Provincia de Salamanca. *Estudios Geológicos* **41**, 301-321.

_____, MARTIN-IZARD, A. & MONTES, J. (1984): Distribución geoquímica del uranio en los metasedimentos del oeste de la provincia de Salamanca. *7th Congreso Internacional de Minería y Metalurgia* (*Barcelona*), *Proc.* **1**, 353-357.

ARTIEDA, J.I., RUIZ, J.& ARNAIZ, J. (1995): A review of the Spanish uranium resources and recent developments in Salamanca province. IAEA Technical Committee Meeting, Kiev, Ukraine.

BINNS, R.A., MCANDREW, J.& SUN, S.S. (1980): Origin of uranium mineralization at Jabiluka. *In* Uranium in the Pine Creek Geosyncline (J. Ferguson & A. B. Goleby, eds.). IAEA, Vienna, Austria (543-562).

BOTH, R., ARRIBAS, A. & SAINT-ANDRÉ, B. (1994): The origin of breccia-hosted uranium deposits in carbonaceous metasediments of the Iberian Peninsula: U–Pb geochronology and stable isotope studies of the Fé deposit, Salamanca province, Spain. *Econ. Geol.* **89**, 584-601.

CUNEY, M., LEROY, J.& PAGEL, M. (1992): *L'uranium.* Presses Universitaires de France, Paris, France.

DAHLKAMP, F.J. (1978):Geologic appraisal of the Key Lake U–Ni deposits, northern Saskatchewan. *Econ. Geol.* **73**, 1430-1449.

_____ & TAN, B. (1977): Geology and mineralogy of the Key Lake U–Ni deposits, northern Saskatchewan, Canada. *In* Geology, Mining and Extractive Processing of Uranium (M.J. Jones, ed.). Inst. Mining Metall., London, U.K. (145-157).

FAYEK, M. & KYSER, T.K. (1997): Characterization of multiple fluid-flow events and rare-earth-element mobility associated with formation of unconformity-type uranium deposits in the Athabasca Basin, Saskatchewan. *Can. Mineral.* **35**, 627-658.

FERNANDEZ-POLO, J.A. (1970): Genesis de los yacimientos uraníferos en metasedimentos de Salamanca (Espana). *In* Panel Proc. Ser., Uranium Exploration Geology. IAEA, Vienna, Austria (243-252).

HARDING, T.P. (1974): Petroleum taps asocciated with wrench faults. *Bull. Am. Assoc. Petroleum Geol.* **58**, 1290-1304.

HARLAND, W.B. (1971): Tectonic transpression in Caledonian Spitsbergen. *Geol. Mag.* **108**, 27-42.

HEGGE, M.R. & ROWNTREE, J.C. (1978): Geologic setting and concepts on origin of uranium deposits in the East Alligator River region, N.T., Australia. *Econ. Geol.* **73**, 1420-1429.

HOEVE, J. (1978): Uranium metallogenic studies; Rabbit Lake, mineralogy and geochemistry. *In* Summary of Investigations (J.E. Christopher & R. Macdonald, eds.). *Saskatchewan Geol. Surv., Misc. Rep.* **78-10**, 61-65.

_____ & QUIRT, D. (1984): Mineralization and host rock alteration in relation to clay mineral diagenesis and evolution of the middle-Proterozoic Athabasca Basin, northern Saskatchewan, Canada. *Saskatchewan Res. Council, Tech. Rep.* **187**.

_____ & _____ (1987): A stationary redox front as a critical factor in the formation of high-grade, unconformity-type uranium ores in the Athabasca Basin, Saskatchewan, Canada. *Bull. Minéral.* **110**, 157-171.

_____ & SIBBALD, T.I.I. (1978): On the genesis of Rabbit Lake and other unconformity-type uranium deposits in northern Saskatchewan, Canada. *Econ. Geol.* **73**, 1450-1473.

_____, _____, RAMAEKERS, P. & LEWRY, J.F. (1980): Athabasca Basin unconformity-type uranium deposits; a special class of sandstone-type deposits? *In* Uranium in the Pine Creek Geosyncline (J. Ferguson & A.B. Goleby, eds.). IAEA, Vienna, Austria (575-594).

JULIVERT, M., FONTBOTÉ, J.M., RIVEIRO, A. & CONDE, L. (1972): Mapa tectónico de la Península Ibérica y Baleares (1:4,000,000). Instituto Geológico y Minero de España, Madrid, Spain.

KNIPPING, H.D. (1971): Geology and uranium metallogenesis, Wollaston lake area, Saskatchewan. *Can. Inst. Mining Metall., Bull.*, **64**(707), 51 (abstr.).

_____ (1974): The concepts of supergene versus hypogene emplacement of uranium at Rabbit Lake, Saskatchewan, Canada. *In* Formation of Uranium Ore Deposits. IAEA, Vienna, Austria (531-549).

KOTZER, T.G. & KYSER. T.K. (1995): Petrogenesis of the Proterozoic Athabasca Basin, northern Saskatchewan, Canada, and its relation to diagenesis, hydrothermal uranium mineralization and paleohydrogeology. *Chem. Geol.* **120**, 45-89.

LITTLE, H.W. (1974): Uranium in Canada. *In* Report of Activities, Part A. *Geol. Surv. Can., Pap.* **74-1**, 137-139.

MARTIN-IZARD, A. (1986): Caracteres tectónicos de los metasedimentos del oeste de la provincia de Salamanca. *Estudios Geológicos* **42**, 415-432.

_____ (1989): *Los yacimientos de uranio en pizarras.* Diputación de Salamanca, Serie Ciencias, 4.

_____, ARIAS, D., FERNANDEZ-RODRIGUEZ, F.J., RUIZ, J. & ARRIBAS, A. (1999): The Fé uranium mine, west central Spain: an Alpine ore deposit developed in a transpressional shear zone. *In* Mineral Deposits: Processes and Processing (C.J. Stanley *et al.*, ed.). Balkema, Rotterdam, The Netherlands (1407-1410).

MATOS DIAS, J.M. & SOARES DE ANDRADE, A.A. (1970): Uranium deposits in Portugal. *In* Uranium Exploration Geology. IAEA, Vienna, Austria (129-142).

MCCREADY, A.J., ANNESLEY, I., PARNELL, J. & RICHARDSON, C. (1999): Uranium bearing carbonaceous matter, McArthur River uranium deposit, Saskatchewan. *In* Summary of investigations 2. *Saskatchewan Geol. Surv., Misc. Rep.* **99-4.2**, 110-120.

MOORE, J.M., ALLEN, P., WELLS, M.K. & HOWLAND, A.F. (1979): Tectonics of the Najd transcurrent fault system, Saudi Arabia. *J. Geol. Soc. London* **136**, 441-454.

OEN ING SOEN (1970): Granite intrusion, folding and metamorphism in central northern Portugal. *Boletin Geologico y Minero de España* **71**, 271-298.

PAGEL, M. (1977): Microthermometry and chemical analysis of fluid inclusions from the Rabbit Lake uranium deposit, Saskatchewan, Canada. *J. Geol. Soc. London* **134**, 392 (abstr.).

RECHES, Z. (1983): Faulting of rocks in three-dimensional strain fields. II. Theoretical analysis. *Tectonophys.* **95**, 133-156.

RUIZ, J., ARNAIZ, J. & ARTIEDA, J.I. (1997a): Evaluación de los yacimientos de uranio del área de Ciudad Rodrigo (Salamanca). *In* Evaluación y diseño de yacimientos minerales. Entorno Gráfico, Madrid, Spain (624-639).

_____, CRIADO, M., CARRETERO, S., BORDONABA, M. & ARTIEDA, J.I. (1997b): La producción de concentrados de uranio en España. Las explotaciones mineras de ENUSA en Ciudad Rodrigo (Salamanca). *Rocas y Minerales* **304**, 66-81.

SANDERSON, A.G. & MARCHINI, W.R.D. (1984): Transpression. *J. Struct. Geol.* **6**, 449-458.

SIBSON, R.H. (1985): Stopping of earthquake ruptures at dilational fault jogs. *Nature* **316**, 248-251.

_____ (1989): *Structure and Mechanics of Fault Zones in Relation to Fault Hosted Mineralization*. Australian Mineral Foundation, Glenside, Australia.

_____, MOORE, J.M. & RANKIN, A.H. (1975): Seismic pumping: a hydrothermal fluid transport mechanism. *J. Geol. Soc. London* **131**, 653-659.

SYLVESTER, A.G. & SMITH, R.R. (1976): Tectonic transpression and basement-controlled deformation in San Andreas fault

zone, Salton Trough, California. *Bull. Am. Assoc. Petroleum Geol.* **60**, 2081- 2102.

VON PECHMAN, E. (1985): Mineralogy of the Key Lake U–Ni orebodies, Saskatchewan, Canada; evidence for their formation by hypogene hydrothermal processes. *In* Geology of Uranium Deposits (T.I.I. Sibbald & W. Petruk, eds.). *Can. Inst. Mining Metall., Spec. Vol.* **32**, 27-37.

WILSON, M.R. & KYSER, T.K. (1987): Stable isotope geochemistry of alteration associated with the Key Lake uranium deposit, Canada. *Econ. Geol.* **82**, 1540-1557.